Eur. Phys. J. D **35**, 261–266 (2005)
DOI: 10.1140/epjd/e2005-00207-5

THE EUROPEAN PHYSICAL JOURNAL D

Low energy electron attachment to C_{60}

V.S. Prabhudesai, D. Nandi, and E. Krishnakumar[a]

Tata Institute of Fundamental Research, Colaba, Mumbai 400 005, India

Received 30 March 2005 / Received in final form 8 June 2005
Published online 2nd August 2005 –

Abstract. Low energy electron attachment to the fullerene molecule (C_{60}) and its temperature dependence are studied in a crossed electron beam–molecular beam experiment. We observe the strongest relative signal of C_{60} anion near 0 eV electron energy with respect to higher energy resonant peaks confirming the contribution of *s*-wave capture to the electron attachment process and hence the absence of threshold behavior or activation barrier near zero electron energy. While we find no temperature dependence for the cross-section near zero energy, we observe a reduction in the cross-sections at higher electron energies as the temperature is increased, indicating a decrease in lifetime of the resonances at higher energies with increase in temperature.

PACS. 34.80.Ht Dissociation and dissociative attachment by electron impact – 34.80.Lx Electron-ion recombination and electron attachment

1 Introduction

Low energy electron capture by the fullerene molecule has been studied by many groups in the last decade including the observation of long lived anion formation (C_{60}^-) through the electron attachment to the fullerene molecule (C_{60}) for the electron energies ranging from close to zero eV to 10 eV. Various techniques like free-electron attachment [1–9], Rydberg electron transfer [4,10,11] and Flowing Afterglow Langmuir Probe (FALP) [12] have been used for such studies.

Although the longevity of the anion product (C_{60}^-) from the above mentioned experiments is well established, there has been a major disagreement in the results from these experiments as far as the close to zero energy electron attachment is concerned. The free-electron attachment experiments by Jaffke et al. [2], Vostrikov et al. [3] Huang et al. [4] and Matejcik et al. [5] as well as the FALP experiment by Smith et al. [12] indicate a threshold for the electron attachment to the fullerene molecule close to zero eV. This threshold had been observed to be in the range of 150 to 260 meV. Tosatti and Manini [13] explained this behavior and estimated the threshold for the low energy electron attachment to C_{60} in the similar range using the symmetry arguments. The arguments ruled out the *s*-wave nature of the electron capture at electron energies close to zero eV. The threshold was obtained using the *p*-wave nature of the capture mechanism. These arguments were based on the oversimplification of the problem in which the inelastic cross-section is substituted by the elastic cross-section [4]. Some of the free electron attachment experiments [1,6–9] as well as the Rydberg electron transfer experiments [4,10,11] indicated the *s*-wave nature of the electron attachment near zero eV. These experiments also showed the absence of an activation barrier in this phenomenon. One of the arguments given for such an absence of a threshold behavior is induced polarization caused in the C_{60} molecule due to the incoming electron. The argument of Tosatti and Manini is countered using the effect of rotational motion of the molecule which makes $L = 0$ state available for the *s*-wave kind of capture [10].

Gianturco and co-workers have studied the resonances in C_{60} in terms of the elastic differential cross-sections [14]. Their quantum scattering calculations indicated that the threshold behaviour of the electron attachment cross-sections may be due to the occurrence of a virtual state from *s-wave* scattering in the a_g symmetry and a peak in the *p-wave* scattering in the t_{1u} symmetry [15]. They have also tried to analyze the single particle resonances in the 2 to 25 eV range in terms of the dynamical trapping behind different centrifugal barriers [16]. Fabrikant and Hotop [17] estimated the relative contribution of *s*-wave and *p*-wave for electron capture cross-section for near zero energy using Vogt-Wannier (V-W) model. They used the high resolution data by Elhamidi et al. [6] and the Rydberg electron attachment rate to estimate the absolute cross-sections near zero energy. Though the data by Elhamidi et al. is supposed to have the highest resolution, the relative intensity of the peak they observed at zero energy is much smaller than that obtained by Vasil'ev et al. [7]. Vostrikov et al. [8] had also reported a relatively higher peak near zero energy (at 0.15 eV) as compared to the attachment cross-sections at higher energies. A neutral beam depletion measurement by Kasperovich et al. [9] also showed

[a] e-mail: ekkumar@tifr.res.in

fairly large relative cross-section at zero energy. Though the most recent measurements [6–9] and the theoretical calculations [17] indicate the presence of the s-wave at near zero energies, there appears to be uncertainty regarding the relative contribution of the s-wave to the overall attachment cross-section as seen in the widely differing relative intensities at zero energy in the experiments [6–9]. In addition, there is the suspected role of temperature of the C_{60} vapor that may be responsible for the observed discrepancies. The role of temperature of the C_{60} vapor has been considered to explain the s-wave attachment near zero energy [7,18]. The argument has been that the population in the A_g ($L = 0$) vibrational state is substantial for temperatures above 600 K making the s-wave capture possible [7]. Considering the discrepancies that exist in the relative cross-sections, we have investigated the electron attachment to C_{60} as a function of temperature. We find that the cross-sections at zero energy to be relatively large as compared to higher energies signifying the dominance of the s-wave attachment. The cross-sections seem to be independent of temperature below 1 eV, though at higher energies there appears to be a systematic decrease with increase in temperature.

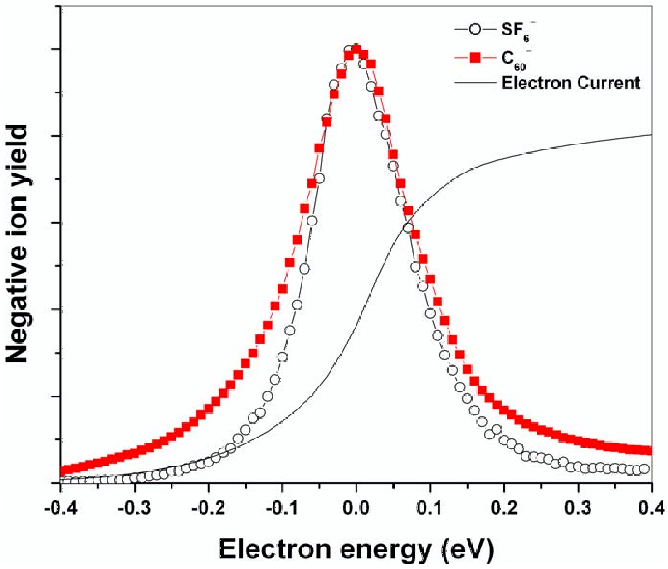

Fig. 1. Comparison of C_{60}^- (squares) signal with that of SF_6^- (circles) collected separately with the electron gun operated in DC mode. The two curves are normalized at the peak. Also given is the current profile of the gun during the run.

2 Experimental

The experiments were carried out in a crossed beam arrangement. The effusive beam of C_{60} vapor was generated by using an oven with a capillary tube in front. The oven temperature was measured using a calibrated thermocouple. The C_{60} beam was made to cross the electron beam at 45° in the plane perpendicular to the flight tube axis. The electron beam was generated using a hot tungsten filament and collimated using a uniform magnetic field of strength 50 Gauss. This magnetic field was generated at the centre of the chamber where the electron gun resides using two identical magnet coils in the Helmholtz geometry. A trochoidal monochromator was used to improve the energy resolution of the electron beam [19]. The interaction point was maintained at the center of the source region of the detection system. The linear Time of Flight (ToF) Mass-spectrometer with the Wiley-McClaren geometry was used for the mass selection of the negative ions [20]. The apertures on the ion extraction electrodes and the flight tube were provided with fine wire mesh for uniformity of the electric field. This also prevented the field penetration in the interaction region from the acceleration region which could affect the energy calibration. A channel electron multiplier operated in the pulse counting mode was used as the ion detector at the end of the 300 mm long flight tube. A shielded and positively biased Faraday cup was used to measure the electron beam current.

Using the time-of-flight mass spectrometer, we confirmed that no negative ion signal is present except that due to C_{60}^- in the electron energy range 0 to 10 eV when only C_{60} vapor beam was present in the interaction region. For the time-of-flight measurement we needed to pulse the electron gun. It was found that this deteriorated the energy resolution of the electron beam. Hence we used the electron gun in the DC mode in order to maintain higher energy resolution. A small DC extraction field (<1 V/cm) was used along with the small flight tube voltage (20 volts) in order to detect the C_{60}^- ions. The spectrum was taken for long enough time to improve the signal to noise ratio.

The energy resolution of the electron beam near zero energy was determined using the full width at half maximum of the SF_6^- peak. The typical energy width of the electron beam was found to be 130 meV when the gun was operated in DC mode with the ions being detected without mass separation. The negative ion signal from SF_6, which is dominated by SF_6^- as a function of electron energy is given in Figure 1 along with the electron beam current. We also give the negative ion signal from C_{60} obtained from identical electron gun conditions. The peaks in both these appear at the same energy. Also the electron current profiles remain almost identical in both cases. A further check on the zero of the electron energy scale for the C_{60}^- excitation function was carried out using a mixture of SF_6 and C_{60}. In this case the electron gun was operated in the pulsed mode so that the two types of ions could be separated using the time-of-flight arrangement. The ion yield curves and the electron beam current were measured simultaneously using the General Purpose Interface Bus (GPIB) based data acquisition system described elsewhere [21]. This mode of operation, though had a poorer energy resolution of 350 meV, confirmed that there is no shift in the peak position of the C_{60}^- as compared to that of SF_6^- signal.

For studying the effect of temperature of the C_{60} vapor on the electron attachment process near zero eV, the

Table 1. Summary of the relative ion yield near zero eV electron energy as compared to that near 1 eV.

Reference	Technique	Oven temperature (K)	Electron energy resolution (meV)	Relative ion yield ($I_{C_{60}^-}$ (0 eV)/$I_{C_{60}^-}$ (1 eV))
1	Free electron attachment	670	200	<1
6	Free electron attachment	725	30	∼1
7	Free electron attachment	673	90	∼7
Our experiment	Free electron attachment	723	130	8.9 ± 0.3

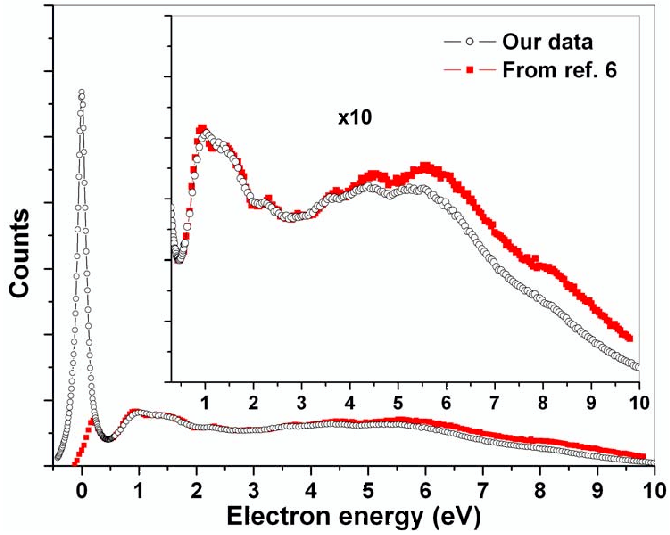

Fig. 2. Plot of C_{60}^- ion yield (circles) as a function of the electron energy taken at 818 K. Also given is the results from reference [6] (squares) after its energy scale is shifted up by 200 meV. The inset shows the same data multiplied by 10. The data are normalized to have the same magnitude at the valley between the first two peaks (please also see text).

excitation function for the C_{60}^- was taken at different oven temperatures in the range from 648 K to 818 K.

3 Results and discussions

The results of our measurements are given in Figure 2 along with the results from Elhamidi et al. [6]. One can clearly see a strong enhancement of the zero eV peak in our data as compared to the higher energy structures. The ratio of intensity of C_{60}^- peak near zero eV to that at higher electron energy (1 eV) was calculated. The result is tabulated in Table 1 along with the ratios from the previously reported experiments.

It appears from the ion yield curves (Fig. 2) that there is no threshold behavior or presence of activation energy for the C_{60}^- ion formation near zero electron energy. Also in spite of the energy resolution of the electron beam on the poorer side as compared to the previously reported experiments, we see the maximum ratio of the intensity of the C_{60}^- ion peak near zero eV to the ion peak at higher energy. Moreover we could obtain all the structures in the higher energy part of the spectrum, which were obtained in the experiment performed using a better electron energy resolution [6], except for a small but systematic difference of 200 meV. We notice that such a shift is present in the extended energy spectrum given by Elhamadi et al. [6] (their Fig. 1) as compared to their own higher resolution data in a smaller energy range (their Fig. 2). Hence in Figure 2 we have shifted their data by 200 meV to the higher energy side. This shift could be justified further by a comparison with other available data [2,3,7]. The shift brings all the high energy peaks in excellent agreement in the two sets of data in Figure 2, with the notable difference being the difference in the zero energy peaks. The difference in the peaks at zero energy may be attributed to the difficulties associated with the use of a pure electrostatic electron gun used by Elhamadi et al. [6].

There may be a question whether the relative intensity of the peak at zero energy as compared to that at higher energies observed in our data is due to increased path-length in the presence of the magnetic field for electrons near zero energy. This is important as the previous results by Vasilev et al. [7] as well as the present one, both showing relatively large zero energy peaks as given in Table 1, were obtained using a magnetically collimated electron beam unlike the case of Elhamidi et al. [6]. In this context we provide the data collected simultaneously on SF_6^- and C_{60}^- by having both target molecules simultaneously present in the interaction region. For this purpose, the electron gun had to be operated in the pulsed mode and hence the energy resolution was poorer. The data thus obtained for the two anions along with the electron gun current profile is given in Figure 3. From a comparison of this figure with that of Figure 2, we note that as the width is reduced by a factor of 2, the relative intensity of the zero energy peak with respect to that at 1 eV of C_{60}^- increases by a factor 2. If the large intensity of the zero energy peak seen in the experiments using magnetic collimation were due to systematic error from increased path-length, the peak height should have increased much faster with improvement in resolution. We note that the zero energy peak in C_{60}^- has a finite width of 150 meV as seen in measurements by Elhamidi et al using an electrostatic gun [6] with an energy resolution of 30 meV and by

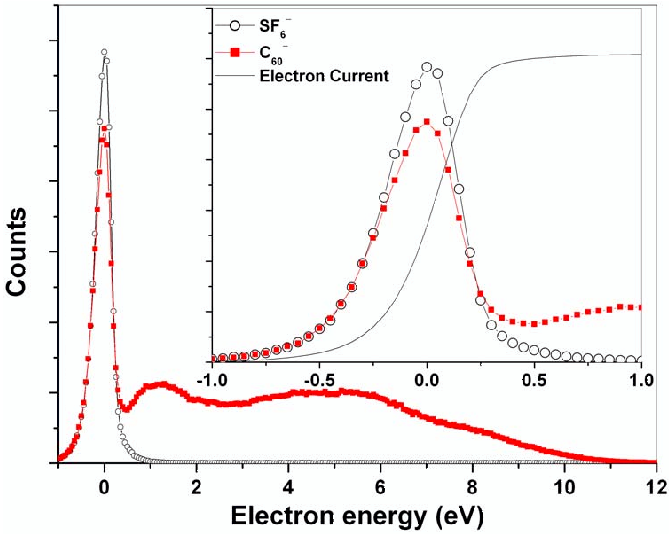

Fig. 3. Comparison of C_{60}^- (squares) signal with that of SF_6^- (circles) in the extended energy scale, collected together with the electron gun operating in pulse mode. The inset shows the electron gun current profile along with both the ion yield curves around zero eV.

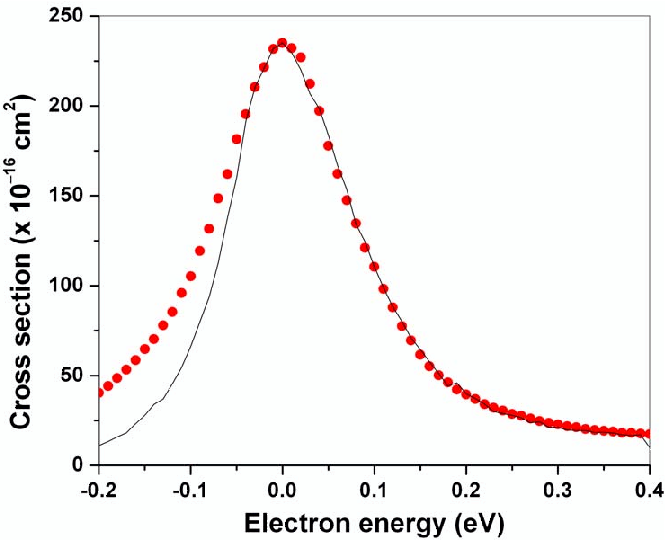

Fig. 4. Comparison of our data (points) at 818 K with the theoretical fit using s-wave and p-wave contributions (Ref. [17]) convoluted with the SF_6^- curve under similar conditions taken as the instrument function. The best fit needed 45% contribution from s-wave to that from p-wave. The cross-sections are normalized to absolute values using the data from Vostrikov et al. [3,8] (see text for details).

Vasilev et al. [7] using a magnetically collimated gun with an energy resolution of 90 meV. We too find a width of 170 meV, though the energy resolution as measured using SF_6^- was about 130 meV. These also point to the fact that the relatively large intensity observed in the experiments using magnetic collimation cannot be due to the increase in path length.

On a different note, the finite width of the peak could be a clear indication of the presence of higher order partial waves contributing to the negative ion signal as described by Fabrikant and Hotop [17]. Although the present electron energy resolution is not good enough to separate out the s-wave contribution from the higher order contributions, the presence of very strong C_{60}^- signal near zero eV despite the poorer energy resolution is indicative enough to support the presence of significant amount of s-wave capture behavior.

Fabrikant and Hotop [17] have used a V-W profile to fit the cross-section measured by Elhamidi et al. since it was the best available data in terms of energy resolution. They calculated the V-W cross-sections for s-wave and p-wave and used the relation $\sigma = c(\varepsilon\sigma_0 + \sigma_1)$, where σ_0 is the s-wave V-W cross-section and σ_1 is the p-wave V-W cross-section and c and ε are adjustable parameters, to determine the total cross-section. They averaged it over a Gaussian profile of 50 meV width and normalized the data by Elhamidi et al. with the theoretical cross-section at 0.2 eV. The best fit gave them a contribution for s-wave about one-tenth of the contribution from p-wave. Though the energy resolutions are poorer, both the data by Vasilev et al. and the present one have larger intensity at the main peak (about a factor of 6 in both cases) as compared to the intensity at 0.2 eV. We have attempted a fit similar to that given by Fabrikant and Hotop [17] by convoluting the SF_6 data (taken here as the instrument function) obtained under similar conditions as that of C_{60} with the s-wave and p-wave cross-sections taken from reference [17]. The fit as shown in Figure 4 gave $\varepsilon = 0.45$, showing considerable contribution due to s-wave. The absolute scale shown in the figure for the cross-sections was determined using the data from Vostrikov et al. [3,8]. It may be noted that there are relatively few measurements of absolute cross-sections for electron attachment to C_{60}. The data by Vostrikov et al. [3,8] show the zero energy peak to be shifted to 0.15 eV with absolute cross-sections of 0.8×10^{-14} cm^2 [3] and 1.2×10^{-14} cm^2 [8]. The beam depletion measurements by Kasperovich et al. [9] give an absolute cross-section of 9×10^{-14} cm^2 at 0.05 eV, though this may be considered an upper limit as it is the total scattering cross-section. Due to the uncertainty in the reliability of the peak position at near-zero energy in Vostrikov et al. [3,8], we normalized our data with the average value of the cross-sections they have reported at 1 eV in the two measurements [3,8], which is 0.34×10^{-14} cm^2. This gives the peak cross-section of 2.4×10^{-14} cm^2 as shown in Figure 3 as against 0.45×10^{-14} cm^2 obtained by Fabrikant and Hotop [17]. By matching this absolute value with the theoretical fit, we get $c = 0.06$.

It is clear from Table 1 that various experiments performed over the period of time have used C_{60} vapor at different temperatures. Hence one of the possible reasons for observing the threshold can be the temperature of the C_{60} vapor not being adequate. We investigated this possibility by carrying out the measurements at various oven temperatures, the results of which are summarized in

Table 2. Relative C_{60}^- ion-yield at different vapor temperatures in the present experiment.

Temperature (K)	Relative ion yield $I_{C_{60}^-}$ (0 eV)/$I_{C_{60}^-}$ (1 eV)
648	09.0 ± 1.8
668	09.0 ± 1.4
723	08.9 ± 0.3
793	08.7 ± 0.2
818	07.0 ± 0.1

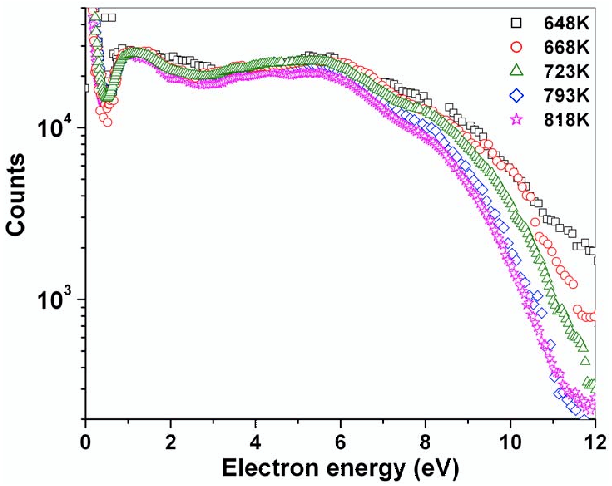

Fig. 5. Plots of C_{60}^- ion yield as a function of the electron energy taken at different C_{60} vapor temperatures. The plots are normalized at the peak near 1 eV. The data at 648, 668 and 723 K were smoothed to reduce the scatter.

Table 2, where we have given the relative intensities of the negative ion signal at electron energy near zero eV to the electron energy at 1 eV. We find that the ratio is independent of the C_{60} vapor temperature, though there is a reduction at 818 K. However the ratio of 7 at this temperature is still much higher than what has been generally reported. We believe that the current measurements rule out the possibility of temperature of the fullerene vapor having played a role in the observed disparity in the earlier measurements.

From the data obtained at different temperatures, we note a decrease in the cross-sections with the increase in temperature at higher electron energies. This could be seen from Figure 5 in which we have plotted the data obtained at various temperatures after normalization at the 1 eV peak. Though at lower temperatures there is large statistical spread, it is seen that the cross-sections decrease with increase in temperature. This may be explained in terms of the decrease in lifetime of the negative ion states formed through electron attachment. The negative ion lifetime at higher temperature could be smaller since it becomes increasingly difficult to dissipate the energy of the incoming electron as many vibrational modes are already saturated at higher temperatures. The autodetachment of C_{60}^- in terms of a model based on thermionic emission has been discussed by Matejčik et al. [5]. This model was used to explain the observed drop in the C_{60}^- intensity at energies above 7 eV for fixed C_{60} temperature. In this model the incident electron energy plus the electron affinity of the C_{60} is assumed to go into exciting the vibrational modes, thereby raising the temperature of the molecule. And as the temperature increases there is increasing autodetachment due to thermionic emission. Based on this model any change in temperature whether due to the energy transferred from the electrons or by direct heating should lead to corresponding changes in the lifetime of the negative ion through the thermionic emission process. Thus our observation of the temperature dependence is consistent with the thermionic emission model given by Matejčik et al. [5]. We also note that the electron capture efficiency has been shown to go down with increase in internal energy of the molecule [6]. This may also add to a reduction in the negative ion signal with increase in temperature. Though one expects to see the temperature dependence at all energies, our data show no noticeable effect at energies below 2 eV. A plausible reason for this could be the temperature (including that transferred from the electron) not being sufficiently large to make noticeable loss due to thermionic emission.

4 Conclusion

We find that the cross-section for electron attachment to C_{60} shows a strong peak at near-zero energies indicating fairly large contribution of the *s*-wave capture in the negative ion formation process. A comparison of all the existing data show that this peak has an inherent width of about 150 meV, indicating contribution from higher order partial waves. We rule out the effect of temperature of the C_{60} vapor as a possible reason for the disparity in earlier reported data. However, the lifetime of the C_{60}^- ions formed by electron capture above 2 eV appears to decrease with increase in temperature and qualitatively support the model of thermionic emission process put forward to explain the decrease in cross-section at larger energies.

We acknowledge the contribution of T.S. Ananthakrishnan (BARC) and S.V.K. Kumar towards the data acquisition program and Satej Tare and Yogesh Upalekar for their technical support. V.S. Prabhudesai and D. Nandi acknowledge the TIFR Alumni Association scholarship from TIFR Endowment fund.

References

1. M. Lezius, P. Scheier, T.D. Mark, Chem. Phys. Lett. **203**, 232 (1993)
2. T. Jaffke, E. Illenberger, M. Lezius, S. Matejcik, D. Smith, T.D. Mark, Chem. Phys. Lett. **226**, 213 (1994)
3. A.A. Vostrikov, D.Yu. Dubnov, A.A. Agarkov, Pis'ma Zh. Tekh. Fiz. **21**, 55 (1995); A.A. Vostrikov, D.Yu. Dubnov, A.A. Agarkov, Tech. Phys. Lett. **21**, 517 (1995)

4. J. Huang, H.S. Carman Jr, R.N. Compton, J. Phys. Chem. **99**, 1719 (1995)
5. S. Matejčik, T.D. Mark, P. Spanel, D. Smith, T. Jaffke, E. Illenberger, J. Chem. Phys. **102**, 2516 (1995)
6. O. Elhamidi, J. Pommier, R. Abouaf, J. Phys. B **30**, 4633 (1997)
7. Y.V. Vasil'ev, R.F. Tuktarov, V.A. Mazunov, Rap. Comm. in Mass Spect. **11**, 757 (1997)
8. A.A. Vostrikov, D.Yu. Dubnov, A.A. Agarkov, High Temp. **39**, 22 (2001)
9. V. Kasperovich, G. Tikhonov, V.V. Kresin, Chem. Phys. Lett. **337**, 55 (2001)
10. C.D. Finch, R.A. Popple, P. Nordlander, F.B. Dunning, Chem. Phys. Lett. **244**, 345 (1995)
11. J.M. Weber, M.W. Ruf, H. Hotop, Z. Phys. D **37**, 351 (1996);
12. D. Smith, P. Spanel, T.D. Märk, Chem. Phys. Lett. **213**, 202 (1993)
13. E. Tosatti, N. Manini, Chem. Phys. Lett. **223**, 61 (1994)
14. F.A. Gianturco, R.R. Lucchese, N. Sanna, J. Phys. B **32**, 2181 (1999)
15. R.R. Lucchese, F.A. Gianturco, N. Sanna, Chem. Phys. Lett. **305**, 413 (1999)
16. F.A. Gianturco, R.R. Lucchese, J. Chem. Phys. **111**, 6769 (1999)
17. I.I. Fabrikant, H. Hotop, Phys. Rev. A **63**, 022706 (2001)
18. M. Lezius, Int. J. Mass Spectrom. **223-224**, 447 (2003)
19. A. Stamatovic, G.J. Schulz, Rev. Sci. Instr. **41**, 423 (1970)
20. W.C. Wiley, I.H. McLaren, Rev. Sci. Instr. **26**, 1150 (1955)
21. D. Nandi, S.A. Rangwala, S.V.K. Kumar, E. Krishnakumar, Int. J. Mass spectrom. **205**, 111 (2001)